



## Original article

# <sup>18</sup>F-Labeled 2-phenylquinoxaline derivatives as potential positron emission tomography probes for *in vivo* imaging of $\beta$ -amyloid plaques

Pingrong Yu<sup>a</sup>, Mengchao Cui<sup>a,\*</sup>, Xuedan Wang<sup>a</sup>, Xiaojun Zhang<sup>b</sup>, Zijing Li<sup>a</sup>, Yanping Yang<sup>a</sup>, Jianhua Jia<sup>a</sup>, Jinming Zhang<sup>b</sup>, Masahiro Ono<sup>c</sup>, Hideo Saji<sup>c</sup>, Hongmei Jia<sup>a</sup>, Boli Liu<sup>a,\*</sup>

<sup>a</sup>Key Laboratory of Radiopharmaceuticals, Ministry of Education, College of Chemistry, Beijing Normal University, Beijing 100875, PR China

<sup>b</sup>Department of Nuclear Medicine, Chinese PLA General Hospital, Beijing 100853, PR China

<sup>c</sup>Department of Patho-Functional Bioanalysis, Graduate School of Pharmaceutical Sciences, Kyoto University, 46-29 Yoshida Shimoadachi-cho, Sakyo-ku, Kyoto 606-8501, Japan

## ARTICLE INFO

## Article history:

Received 16 June 2012

Received in revised form

14 July 2012

Accepted 23 August 2012

Available online 1 September 2012

## Keywords:

Alzheimer's disease

$\beta$ -Amyloid plaque

2-Phenylquinoxaline

Autoradiography

Biodistribution

## ABSTRACT

In continuation of our study on the 2-phenylquinoxaline scaffold as potential  $\beta$ -amyloid imaging probes, two [<sup>18</sup>F]fluoro-pegylated 2-phenylquinoxaline derivatives, 2-(4-(2-[<sup>18</sup>F]fluoroethoxy)phenyl)-N-methylquinoxalin-6-amine ([<sup>18</sup>F]**4a**) and 2-(4-(2-(2-(2-[<sup>18</sup>F]fluoroethoxy)ethoxy)ethoxy)phenyl)-N-methylquinoxalin-6-amine ([<sup>18</sup>F]**4b**) were prepared. Both of them displayed high binding affinity to A $\beta$ <sub>1-42</sub> aggregates ( $K_i = 10.0 \pm 1.4$  nM for **4a**,  $K_i = 5.3 \pm 3.2$  nM for **4b**). The specific and high binding of [<sup>18</sup>F]**4a** and [<sup>18</sup>F]**4b** to A $\beta$  plaques was confirmed by *in vitro* autoradiography on brain sections of AD human and transgenic mice. In biodistribution in normal mice, [<sup>18</sup>F]**4a** displayed high initial brain uptake (8.17% ID/g at 2 min) and rapid washout from the brain. These preliminary results suggest [<sup>18</sup>F]**4a** may be a potential PET imaging agent for A $\beta$  plaques in the living human brain.

© 2012 Elsevier Masson SAS. All rights reserved.

## 1. Introduction

Alzheimer's disease (AD) is the most common senile dementia. AD patients suffer from growing dementia and disability including cognitive decline, irreversible memory loss, disorientation, and language impairment, which are because of the progressive neurodegeneration in the brain. Till now, there is no effective therapeutic method for AD, however, the rapid growing of AD population has brought a ruin to not only the AD patients but also their families. AD is histopathologically characterized by  $\beta$ -amyloid (A $\beta$ ) plaques and neurofibrillary tangles, which presents in the gray matter of AD patient even before the dementia [1–3]. In addition, A $\beta$  plaques had not been found in other kinds of dementia such as frontotemporal dementia or pure vascular dementia [4]. At this point of view, *in vivo* detection of A $\beta$  plaques in the brain by positron emission tomography (PET) should be useful for early diagnosis of AD [5–8].

In the past decades, a number of PET imaging probes for A $\beta$  plaques have been reported, several of which have been reported for clinical trials. The first A $\beta$  plaques tracer for PET is

2-(4-([<sup>11</sup>C]methylamino)phenyl)-6-hydroxybenzothiazol ([<sup>11</sup>C]PIB,  $K_i = 0.87 \pm 0.18$  nM) [9,10], a neutral analog of thioflavin-T. After that, other <sup>11</sup>C-labeled A $\beta$  imaging agents such as 4-N-[<sup>11</sup>C]methylamino-4'-hydroxystilbene ([<sup>11</sup>C]SB-13,  $K_i = 6.0 \pm 1.5$  nM) [11,12] and 2-[6-([<sup>11</sup>C]methylamino)pyridin-3-yl]-1,3-benzothiazol-6-ol ([<sup>11</sup>C]AZD2184,  $K_i = 1.70 \pm 0.54$  nM) [13–15] had also been reported under clinical trials and displayed effective result in differentiating AD patients with controls by measuring the brain uptake and retention. As a <sup>11</sup>C-labeled tracer, the chemical structure is retained, which completely maintained the biological property of molecular. But the short half-life of <sup>11</sup>C ( $t_{1/2} = 20$  min) leads to that the supply of <sup>11</sup>C-labeled tracers will be limited to centers equipped with an on-site cyclotron, which may be the most important reason for preventing <sup>11</sup>C-labeled tracers to be more widely used. Meanwhile, <sup>18</sup>F ( $t_{1/2} = 110$  min) has a longer radioactive decay half-life, which permits a more widespread application, and allowed multiple injections from a single production batch. In this case, <sup>18</sup>F may be the better radionuclide for PET imaging. Great efforts have been focused on the development of <sup>18</sup>F-labeled A $\beta$  plaques tracers. Some of them like 4-(N-methylamino)-4'-(2-(2-[<sup>18</sup>F]fluoroethoxy)ethoxy)ethoxy)-stilbene ([<sup>18</sup>F]BAY94-9172, florbetaben,  $K_i = 2.22 \pm 0.54$  nM) [16,17], 2-(3-[<sup>18</sup>F]fluoro-4-methylaminophenyl)benzothiazol-6-ol ([<sup>18</sup>F]GE-067, flutemetamol,  $K_i = 0.74 \pm 0.38$  nM) [18] had already been reported under clinical

\* Corresponding authors. Tel./fax: +86 10 58808891.

E-mail addresses: [cmc@bnu.edu.cn](mailto:cmc@bnu.edu.cn) (M. Cui), [liuboli@bnu.edu.cn](mailto:liuboli@bnu.edu.cn) (B. Liu).

trials. In April 2012, (*E*)-4-(2-(6-(2-(2-(<sup>18</sup>F)fluoroethoxy)ethoxy)ethoxy)pyridin-3-yl)vinyl)-*N*-methylaniline ([<sup>18</sup>F]AV-45, florbeta-pir,  $K_i = 2.87 \pm 0.17$  nM) [19–21], had been approved by the U.S. Food and Drug Administration (FDA) as a radioactive diagnostic agent indicated for brain imaging of A $\beta$  plaques in patients who are being evaluated for AD and other causes of cognitive impairment.

However, clinical trials for <sup>18</sup>F-labeled A $\beta$  imaging tracers show that there is greater white matter retention compared with <sup>11</sup>C-labeled agents, and high non-specific white matter retention may limit the sensitivity of PET imaging. The mechanism of white matter retention seems to be owing to non-specific binding [22], besides further modifications in order to decrease lipophilicity are needed. In addition, almost all of the tracers evaluated in humans are thioflavin-T or stilbene derivatives. Thus, development of tracers with a new scaffold may lead a new way to improve the *in vivo* properties including higher affinity to A $\beta$  plaques and less nonspecific binding in the white matter of the brain.

In a search for novel A $\beta$  imaging probes, we have recently reported a lipophilic <sup>125</sup>I-labeled 2-phenylquinoxaline derivative ([<sup>125</sup>I]QN-1) [23], which displayed high affinity to A $\beta$  aggregates ( $K_i = 4.1 \pm 0.7$  nM). Film autoradiography and fluorescent staining confirmed the specific binding to A $\beta$  plaques on postmortem AD brain sections. In biodistribution experiment, this probe exhibited high initial uptake into the brain (6.03% ID/g at 2 min), but unsatisfactory rate of washing out (2.98% ID/g at 60 min). This may be caused by its high lipophilicity (LogD = 4.02) due to the existence of iodine atom. To improve the pharmacokinetic profile of [<sup>125</sup>I]QN-1 for using as a PET imaging agent, the iodine atom was replaced by a short fluorine end-capped polyethylene glycol chain ( $n = 1$  or 3) [24]. Furthermore, aiming of circumventing the problem of the rapid *in vivo* *N*-demethylation for dimethylamino group which appeared in metabolism of tracers like 6-[<sup>123</sup>I]iodo-2-(4'-dimethylamino)-phenyl-imidazo [1,2] pyridine ([<sup>123</sup>I]IMPY) [25–27] and (*E*)-4-(2-(6-(2-(2-(<sup>18</sup>F)fluoroethoxy)ethoxy)ethoxy)pyridin-3-yl)vinyl)-*N,N*-dimethylaniline ([<sup>18</sup>F]AV-19) [7], most of the radiotracers for A $\beta$  plaques in clinical trials have a monomethylamino group. Accounting for the same reason, the dimethylamino group in [<sup>125</sup>I]QN-1 was changed to monomethylamino group.

In the present study, we reported the synthesis and evaluation of novel <sup>18</sup>F-labeled 2-phenylquinoxaline probes for A $\beta$  plaques with fluoro-pegylated side chains of different length ( $n = 1$  or 3) and a monomethylamino group, expecting of better *in vivo* properties comparing with the radioiodinated ligand (Figs. 1 and 2).

## 2. Results and discussion

### 2.1. Chemistry

The synthesis was shown in Scheme 1 and Scheme 2. The derivative **1** was formed by a one-pot tandem oxide condensation procedure in DMSO (yield 93.6%). The amino derivative **2** was obtained from **1** by reduction with excess hydrazine hydrate in

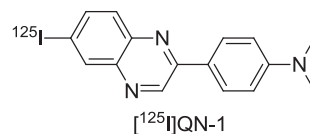


Fig. 2. Chemical structure of 2-phenylquinoxaline derivative [<sup>125</sup>I]QN-1.

ethanol in which Pd/C was added as catalyzer (yield 95.6%). Monomethylation of derivative **2** was achieved with paraformaldehyde, sodium methoxide and sodium borohydride to obtain derivative **3** (yield 88.7%). The corresponding fluoropegylated derivative **4a**, **4b** were prepared by **3** with K<sub>2</sub>CO<sub>3</sub>, 1-bromo-2-fluoroethane or 2-(2-(2-fluoroethoxy)ethoxy)ethyl 4-methylbenzenesulfonate in DMF (yield 51.8%, 35.0%). Ethane-1,2-diyl bis(4-methylbenzenesulfonate) or (ethane-1,2-diylbis(oxy))bis(ethane-2,1-diyl) bis(4-methylbenzenesulfonate) was coupled with the hydroxy group of **3** with K<sub>2</sub>CO<sub>3</sub> and 18-crown-6 in acetone to obtain **5a**, **5b** (yield 27.5%, 73.6%). The tosylate precursor **6a** and **6b** were obtained by protecting the methylamino groups of **5a** and **5b** with di-tert-butylidicarbonate in THF (yield 43.1%, 52.6%).

### 2.2. Radiolabeling

To get the radiofluorinated ligands [<sup>18</sup>F]**4a**, [<sup>18</sup>F]**4b**, the *N*-BOC-protected tosylate precursor **6a**, **6b** was mixed with [<sup>18</sup>F]fluoride, potassium carbonate and Kryptofix 222 in acetonitrile under heating at 110 °C for 5 min. The mixtures were treated with aqueous hydrochloric acid to remove the *N*-BOC-protecting group, and neutralized by sodium dicarbonate. The mixture was loaded on a Sep-Pak Plus-C18 cartridge (Waters), and the elution was concentrated and the residue was purified by HPLC. The <sup>18</sup>F-labeled [<sup>18</sup>F]**4a** and [<sup>18</sup>F]**4b** were prepared with an average radiochemical yield of 20% and 52% (no decay corrected), and radiochemical purity of >98%. The identity of [<sup>18</sup>F]**4a** and [<sup>18</sup>F]**4b** was verified by a comparison of the retention time with that of the nonradioactive compound (Fig. 3), and their specific activity was estimated at approximately 200 GBq/μmol.

### 2.3. Biological evaluation

To evaluate the binding affinity of the two 2-phenylquinoxaline derivatives (**4a** and **4b**) to A $\beta_{1-42}$  aggregates, *in vitro* inhibition assay was carried out in solutions with [<sup>125</sup>I]IMPY as the competing radioligand according to conventional methods [28]. The result is shown in Table 1. As expected, the two derivatives showed good binding affinity to A $\beta_{1-42}$  aggregates ( $K_i = 10.0 \pm 1.4$  nM for **4a**,  $K_i = 5.3 \pm 3.2$  nM for **4b**) comparable to the value determined under the same assay system for IMPY ( $K_i = 10.5 \pm 1.0$  nM). Compared with the iodinated tertiary *N,N*-dimethylamino analog QN-1 ( $K_i = 4.1 \pm 0.7$  nM), these fluorinated secondary monomethylamino analogs still kept the high affinity.

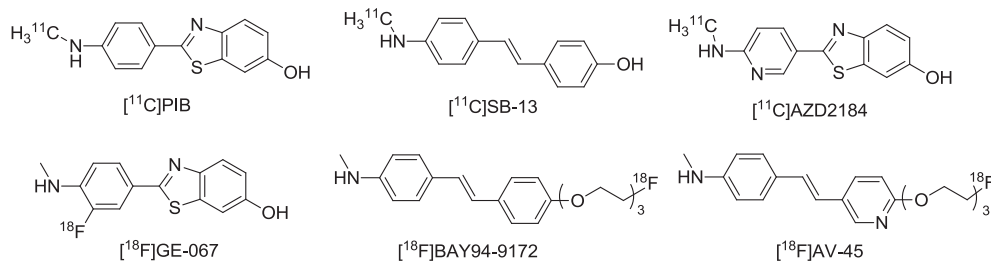
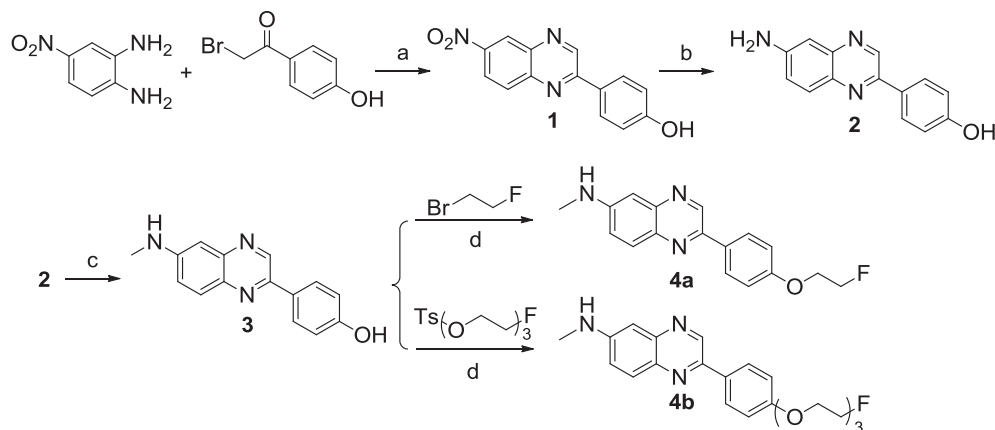


Fig. 1. Chemical structure of reported A $\beta$  imaging probes for clinical trials.



**Scheme 1.** Synthesis of the fluoropegylated phenylquinoxaline derivatives **4a** and **4b**. Reagents and conditions: a. DMSO, rt; b.  $\text{N}_2\text{H}_4 \cdot \text{H}_2\text{O}$ , Pd/C, EtOH, reflux; c. (1)  $(\text{HCHO})_n$ ,  $\text{CH}_3\text{ONa}$ , reflux; (2)  $\text{NaBH}_4$ , reflux; d.  $\text{K}_2\text{CO}_3$ , DMF,  $110^\circ\text{C}$ .

The  $\log D$  values ( $3.14 \pm 0.23$  for  $[^{18}\text{F}]\mathbf{4a}$ ,  $2.79 \pm 0.14$  for  $[^{18}\text{F}]\mathbf{4b}$  and  $4.02 \pm 0.12$  for  $[^{125}\text{I}]\text{QN-1}$ ) showed in Table 3 confirm that the importing of fluoropegylated chain is an effective path to decrease the lipophilicity of the tracers. The lipophilicity was reduced as the length of the fluoro-pegylated chain being increased, which may lower the non-specific binding in brain (Fig. 4).

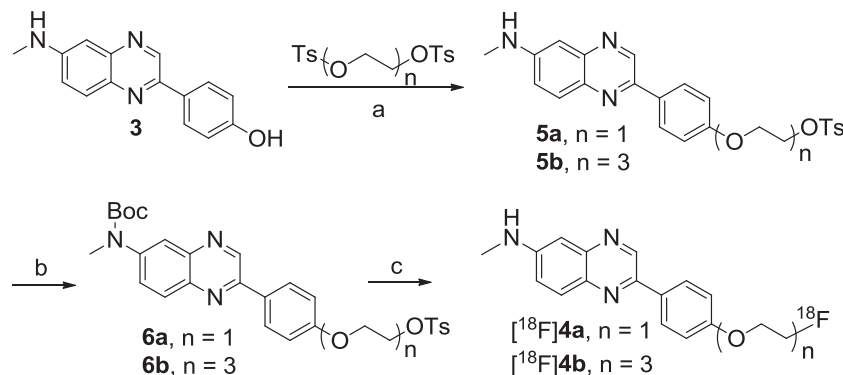
*In vitro* autoradiography in sections of brain tissue from AD patients or Tg model mice (C57BL/6, APPswe/PSEN1, 12 months old) was carried out to confirm the high binding affinity of  $[^{18}\text{F}]\mathbf{4a}$  and  $[^{18}\text{F}]\mathbf{4b}$  to  $\text{A}\beta$  plaques. As shown in Fig. 5A and C, specific labeling of plaques was observed in the brain sections of transgenic mice. The presence and distribution of  $\text{A}\beta$  plaques was consistent with the results of fluorescent staining using thioflavin-S on the same sections (Fig. 5B and D). Furthermore, intense labeling of plaques and low non-specific background were observed in the brain sections of AD patients (Fig. 6A and B). In contrast, no apparent labeling was observed in normal adult brain sections (Fig. 6C and D).

Biodistribution experiments in normal male ICR mice were carried out to evaluate the ability of radiofluorinated tracers ( $[^{18}\text{F}]\mathbf{4a}$  and  $[^{18}\text{F}]\mathbf{4b}$ ) to penetrate the blood–brain barrier (BBB) and properties of clearance from the brain. As shown in Tables 2 and 3,  $[^{18}\text{F}]\mathbf{4a}$  with a short ( $n = 1$ ) fluoro-pegylated side chain displayed a higher initial brain uptake (8.17% ID/g at 2 min) than that of  $[^{18}\text{F}]\mathbf{4b}$  with a long ( $n = 3$ ) side chain (2.49% ID/g at 2 min). The lower brain uptake for  $[^{18}\text{F}]\mathbf{4b}$  may be due to more hydrogen bonds formed between the longer fluoro-pegylated chain and water or other biomolecules *in vivo* which decrease the initial brain uptake.

Compared with  $[^{125}\text{I}]\text{QN-1}$  (6.03% ID/g at 2 min) and  $[^{18}\text{F}]\text{AV-45}$  (7.33% ID/g at 2 min), the initial brain uptake of  $[^{18}\text{F}]\mathbf{4a}$  is superior. High initial brain uptake and high  $\text{brain}_{2\text{ min}}/\text{brain}_{60\text{ min}}$  ratio in normal mouse brain are considered to be important as *in vivo* pharmacokinetic indexes for selecting appropriate  $\text{A}\beta$  imaging tracers. As shown in Table 3, the  $\text{brain}_{2\text{ min}}/\text{brain}_{60\text{ min}}$  ratio is 2.58, 3.89, 2.07, 3.90 for  $[^{18}\text{F}]\mathbf{4a}$ ,  $[^{18}\text{F}]\mathbf{4b}$ ,  $[^{125}\text{I}]\text{QN-1}$ , and  $[^{18}\text{F}]\text{AV-45}$ , respectively. The ratios of  $[^{18}\text{F}]\mathbf{4a}$  and  $[^{18}\text{F}]\mathbf{4b}$  are obviously higher than that of  $[^{125}\text{I}]\text{QN-1}$ , this may due to the introduction of fluoro-pegylated chains which reduce the lipophilicity of these two probes.  $[^{18}\text{F}]\mathbf{4a}$  and  $[^{18}\text{F}]\mathbf{4b}$  also distributed to several other organs. The liver and kidney showed an initial uptake with washout, continuous gastrointestinal accumulation of the radiotracers resulted in an intestine uptake (18.75% ID/g and 39.02% ID/g at 60 min). In addition, accumulation of radioactivity in the bone, 2.46% ID/g observed already at 2 min pi and steadily increased up to 6.20% ID/g during the course of the experiment, suggesting little defluorination *in vivo* of  $[^{18}\text{F}]\mathbf{4a}$ , while the bone uptake of  $[^{18}\text{F}]\mathbf{4b}$  remained almost constant, indicating no defluorination *in vivo*.

### 3. Conclusion

In conclusion, two novel 2-phenylquinoxaline derivatives containing an end-capped fluoro-pegylated chains ( $n = 1, 3$ ) had been successfully prepared and evaluated as PET imaging tracers for  $\text{A}\beta$  plaques. These two compounds appeared to have good binding affinities to  $\text{A}\beta$  aggregates.  $[^{18}\text{F}]\mathbf{4a}$  with a short fluoro-pegylated chain ( $n = 1$ ) displayed a high initial brain uptake and good ratio



**Scheme 2.** Synthesis of the precursors and radiolabeling. Reagents and conditions: a.  $\text{K}_2\text{CO}_3$ , acetone, 18-crown-6, reflux; b.  $(\text{Boc})_2\text{O}$ , THF; c. (1) Kryptofix 222,  $\text{K}_2\text{CO}_3$ ,  $^{18}\text{F}^-$ ,  $\text{CH}_3\text{CN}$ ,  $100^\circ\text{C}$ ; (2) 1 M HCl,  $100^\circ\text{C}$ .

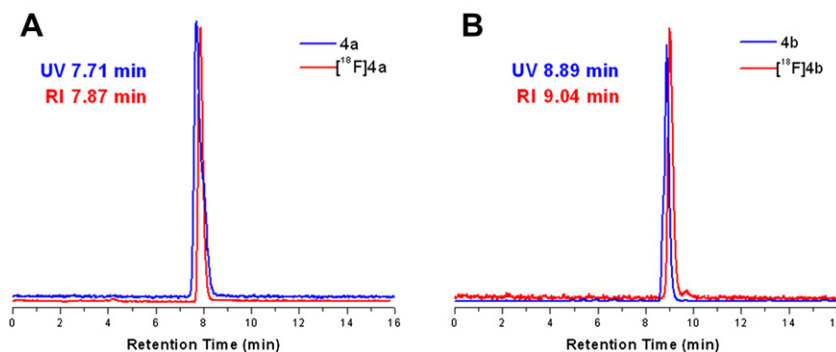


**Fig. 3.** HPLC profiles of **4a**, [ $^{18}\text{F}$ ]**4a** (A) and **4b**, [ $^{18}\text{F}$ ]**4b** (B). HPLC conditions: Venusil MP C18 column (Agela Technologies,  $10 \times 250$  mm),  $\text{CH}_3\text{CN}/\text{H}_2\text{O} = 80/20$  for **4a**,  $\text{CH}_3\text{CN}/\text{H}_2\text{O} = 70/30$  for **4b**, 4 mL/min, UV, 254 nm.

of  $\text{brain}_{2 \text{ min}}/\text{brain}_{60 \text{ min}}$ , and the *in vitro* autoradiography studies confirmed its specific binding to  $\text{A}\beta$  plaques and low non-specific binding, which suggests [ $^{18}\text{F}$ ]**4a** may be a potential PET imaging agent for *in vivo* detection of  $\text{A}\beta$  plaques.

## 4. Experimental

### 4.1. General information

All reagents used in the synthesis were commercial products and were used without further purification unless otherwise indicated.  $^{18}\text{F}^-$  was obtained from the Chinese PLA General Hospital. The  $^1\text{H}$  NMR spectra were obtained at 400 MHz on Bruker spectrometer in  $\text{CDCl}_3$  or  $[\text{D}_6]-\text{DMSO}$  at room temperature with TMS as an internal standard. Chemical shifts were reported as  $\delta$  values with respect to residual solvents. The multiplicity is defined by s (singlet), d (doublet), t (triplet), m (multiplet). Mass spectrometry was acquired under the Surveyor MSQ Plus (ESI) (Waltham, MA, USA) instrument. Reactions were monitored by TLC (precoated silica gel plate F254, Merck). Radiochemical purity was determined by HPLC performed on a Shimadzu SCL-20 AVP equipped with a Bioscan Flow Count 3200 NaI/PMT  $\gamma$ -radiation scintillation detector. Separations were achieved on a Venusil MP C18 column (Agela Technologies,  $10 \mu\text{m}$ ,  $10 \text{ mm} \times 250 \text{ mm}$ ) eluted with a binary gradient system at a 4.0 mL/min flow rate. Mobile phase A was water while mobile phase B was acetonitrile. Fluorescent observation was performed by the LSM 510 META (Zeiss, Germany) equipped with a LP 505 filter set (excitation, 405 nm; long-pass filter, 505 nm). The purity of the synthesized key compounds was determined using analytical HPLC and was found to be more than 95%. ICR Mice (five weeks, 20–22 g, male) were used for biodistribution experiments. All protocols requiring the use of mice were approved by the animal care committee of Beijing Normal University. Postmortem brain tissues from an autopsy-confirmed case of AD (5  $\mu\text{m}$ , temporal lobe) and a control subject (5  $\mu\text{m}$ , temporal lobe) were obtained from BioChain Institute Inc.

**Table 1**

Inhibition constants ( $K_i$ ) for binding to aggregates of  $\text{A}\beta_{1-42}$  versus [ $^{125}\text{I}$ ]IMPY.<sup>a</sup>

Compound	$K_i$ (nM)
<b>4a</b>	$10.0 \pm 1.4$
<b>4b</b>	$5.3 \pm 3.2$
QN-1 <sup>b</sup>	$4.1 \pm 0.7$
IMPY <sup>b</sup>	$10.5 \pm 1.0$

<sup>a</sup> Measured in triplicate with results given as the mean  $\pm$  SD.

<sup>b</sup> Data from literature [23].

Transgenic mice brain tissues (C57BL6, APP<sup>sw</sup>/PSEN1, 12 months old, male) were purchased from Institute of Laboratory Animal Sciences, Chinese Academy of Medical Sciences.

### 4.2. 4-(6-Nitroquinoxalin-2-yl)phenol (**1**)

A mixture of 2-bromo-1-(4-hydroxyphenyl)ethanone (1 mmol) and 4-nitrobenzene-1,2-diamine (1 mmol) was stirred in 5 mL DMSO at room temperature. The reaction mixture was poured into water, and quickly filtered over a buchner funnel. The filter residue was washed with water, oven dried and purified by silica gel chromatography (petroleum ether/ethylacetate = 2:1), to give 250 mg of **1** in a yield of 93.6%.  $^1\text{H}$  NMR (400 MHz,  $[\text{D}_6]-\text{DMSO}$ )  $\delta$  10.27 (s, 1H), 9.68 (d,  $J = 4.5$  Hz, 1H), 8.81 (dd,  $J = 13.2, 2.5$  Hz, 1H), 8.50 (dd,  $J = 9.2, 2.6$  Hz, 1H), 8.29 (d,  $J = 8.8$  Hz, 2H), 8.23 (t,  $J = 9.0$  Hz, 1H), 6.98 (d,  $J = 8.7$  Hz, 2H), 5.37 (s, 1H). MS (ESI)  $m/z$  calcd for  $\text{C}_{14}\text{H}_9\text{N}_3\text{O}_3$  267.1, found 267.7  $[\text{M} + \text{H}]^+$ .

### 4.3. 4-(6-Aminoquinoxalin-2-yl)phenol (**2**)

A mixture of compound **1** (2 mmol) and hydrazine hydrate (8 mmol) in ethanol (20 mL) was refluxed over night, in which Pd/C

**Table 2**

Biodistribution of in ICR normal mice after iv injections of [ $^{18}\text{F}$ ]tracers (% ID/g, Mean  $\pm$  SD,  $n = 5$ ).

	2 min	10 min	30 min	60 min
[ $^{18}\text{F}$ ] <b>4a</b> (LogD = $3.14 \pm 0.23$ )				
Blood	$4.93 \pm 0.43$	$4.68 \pm 0.32$	$5.09 \pm 0.30$	$5.24 \pm 0.45$
Brain	$8.17 \pm 1.33$	$5.07 \pm 0.71$	$3.45 \pm 0.13$	$3.17 \pm 0.22$
Heart	$6.08 \pm 0.37$	$4.27 \pm 0.60$	$4.28 \pm 0.54$	$4.24 \pm 0.22$
Liver	$9.50 \pm 1.04$	$7.80 \pm 1.33$	$5.37 \pm 0.51$	$5.00 \pm 0.84$
Spleen	$4.71 \pm 0.17$	$3.87 \pm 0.57$	$3.35 \pm 0.50$	$3.04 \pm 0.64$
Lung	$6.38 \pm 0.79$	$4.36 \pm 0.42$	$3.78 \pm 0.56$	$3.77 \pm 0.36$
Kidney	$9.37 \pm 1.11$	$5.96 \pm 0.42$	$4.25 \pm 0.43$	$3.79 \pm 0.66$
Bone	$2.46 \pm 0.73$	$2.84 \pm 0.54$	$5.73 \pm 0.29$	$6.20 \pm 0.25$
Stomach <sup>a</sup>	$1.81 \pm 0.42$	$2.55 \pm 0.54$	$1.84 \pm 0.36$	$2.50 \pm 1.19$
Intestine <sup>a</sup>	$9.63 \pm 1.10$	$12.87 \pm 2.61$	$17.15 \pm 1.23$	$18.75 \pm 3.90$
[ $^{18}\text{F}$ ] <b>4b</b> (LogD = $2.79 \pm 0.14$ )				
Blood	$5.51 \pm 0.34$	$3.32 \pm 0.32$	$2.38 \pm 0.21$	$1.54 \pm 0.12$
Brain	$2.49 \pm 0.22$	$1.44 \pm 0.11$	$0.83 \pm 0.17$	$0.64 \pm 0.07$
Heart	$3.21 \pm 0.46$	$1.76 \pm 0.19$	$1.19 \pm 0.19$	$1.03 \pm 0.15$
Liver	$14.18 \pm 1.66$	$14.09 \pm 1.49$	$7.90 \pm 1.07$	$4.89 \pm 0.74$
Spleen	$2.07 \pm 0.97$	$1.65 \pm 0.11$	$1.21 \pm 0.21$	$0.94 \pm 0.39$
Lung	$4.07 \pm 0.45$	$2.40 \pm 0.33$	$1.76 \pm 0.25$	$1.15 \pm 0.11$
Kidney	$5.52 \pm 0.46$	$3.91 \pm 0.27$	$3.27 \pm 0.74$	$1.65 \pm 0.94$
Bone	$1.49 \pm 0.34$	$1.00 \pm 0.40$	$1.12 \pm 0.23$	$1.78 \pm 0.06$
Stomach <sup>a</sup>	$1.55 \pm 0.12$	$2.81 \pm 1.31$	$3.21 \pm 1.62$	$6.53 \pm 2.03$
Intestine <sup>a</sup>	$6.06 \pm 0.64$	$12.26 \pm 2.94$	$32.83 \pm 6.30$	$39.02 \pm 6.98$

<sup>a</sup> Expressed as % ID.

**Table 3**

Comparison of inhibition constants ( $K_i$ ) and brain kinetics between radiolabeled 2-phenylquinoxaline derivatives and [ $^{18}\text{F}$ ]AV-45.

Compound	$K_i$ (nM)	Brain $_2$ min <sup>a</sup>	Ratio $_{\text{O}_2}$ min/60 min	LogD
[ $^{18}\text{F}$ ]4a	10.0	8.17	2.58	3.14
[ $^{18}\text{F}$ ]4b	5.3	2.49	3.89	2.79
[ $^{125}\text{I}$ ]QN-1 <sup>b</sup>	4.1	6.03	2.07	4.02
[ $^{18}\text{F}$ ]AV-45 <sup>c</sup>	2.9	7.33	3.90	2.41

<sup>a</sup> Expressed as % ID/g.

<sup>b</sup> Data from literature [23].

<sup>c</sup> Data from literature [19].

was added as catalyzer. The reaction mixture was cooled to room temperature and then filtered. The filtrate was concentrated, and purified by silica gel chromatography (petroleum ether/ethylacetate = 1:1) to give 453 mg of **2** in a yield of 95.6%.  $^1\text{H}$  NMR (400 MHz, [ $\text{D}_6$ ]-DMSO)  $\delta$  9.86 (s, 1H), 9.21 (s, 1H), 8.10 (d,  $J$  = 8.7 Hz, 2H), 7.78 (d,  $J$  = 9.0 Hz, 1H), 7.28 (dd,  $J$  = 9.0, 2.4 Hz, 1H), 6.99 (d,  $J$  = 2.4 Hz, 1H), 6.98 (s, 1H), 6.95 (s, 1H), 6.03 (s, 2H). MS (ESI)  $m/z$  calcd for  $\text{C}_{14}\text{H}_{11}\text{N}_3\text{O}$  237.1, found 237.7 [M + H]<sup>+</sup>.

#### 4.4. 4-(6-(Methylamino)quinoxalin-2-yl)phenol (**3**)

A solution of compound **3** (2.3 mmol) in methanol (20 mL) was added with sodium methoxide (4.5 mmol) and paraformaldehyde (9 mmol). The reaction mixture was refluxed for 2 h then cooled to 0 °C in an ice bath. Sodium borohydride (9 mmol) was added carefully. The mixture was refluxed again for 1 h and cooled to room temperature. After solvent being removed in vacuo, water (10 mL) was added, and then ethylacetate (3 × 50 mL) was used for extraction. The organic phase was dried over  $\text{MgSO}_4$ , and concentrated latter. The residue was purified by silica gel chromatography (petroleum ether/ethylacetate = 1:1) to give 512 mg of **3** in a yield of 88.7%.  $^1\text{H}$  NMR (400 MHz, [ $\text{D}_6$ ]-DMSO)  $\delta$  9.80 (s, 1H), 9.18 (s, 1H), 8.05 (d,  $J$  = 8.7 Hz, 2H), 7.74 (d,  $J$  = 9.1 Hz, 1H), 7.25 (dd,  $J$  = 9.1, 2.5 Hz, 1H), 6.91 (d,  $J$  = 8.6 Hz, 2H), 6.74 (d,  $J$  = 2.4 Hz, 1H), 2.83 (s, 3H). MS (ESI)  $m/z$  calcd for  $\text{C}_{15}\text{H}_{13}\text{N}_3\text{O}$  251.1, found 251.8 [M + H]<sup>+</sup>.

#### 4.5. 2-(4-(2-Fluoroethoxy)phenyl)-N-methylquinoxalin-6-amine (**4a**)

A mixture of compound **3** (0.35 mmol) and 1-bromo-2-fluoroethane (0.5 mmol) in DMF (5 mL) was refluxed for 2 h. After being cooled to room temperature, water (10 mL) and  $\text{CH}_2\text{Cl}_2$  (20 mL) were added to the mixture. The organic layer was separated, washed with water (3 × 10 mL), and dried over  $\text{MgSO}_4$ . The solvent was removed in vacuo, and the residue was purified by silica gel chromatography (petroleum ether/ethylacetate = 2:1) to

give 54 mg of **4a** in a yield of 51.8%.  $^1\text{H}$  NMR (400 MHz,  $\text{CDCl}_3$ )  $\delta$  9.10 (s, 1H), 8.08 (d,  $J$  = 8.8 Hz, 2H), 7.87 (d,  $J$  = 9.1 Hz, 1H), 7.13 (dd,  $J$  = 9.1, 2.6 Hz, 1H), 7.08 (d,  $J$  = 8.8 Hz, 2H), 6.98 (d,  $J$  = 2.5 Hz, 1H), 4.89–4.85 (m, 1H), 4.77–4.73 (m, 1H), 4.35–4.33 (m, 1H), 4.28–4.25 (m, 1H), 3.00 (s, 3H).  $^{13}\text{C}$  NMR (100 MHz,  $\text{CDCl}_3$ )  $\delta$  159.50, 149.80, 147.20, 143.75, 142.77, 137.12, 130.77, 130.02, 128.27, 122.07, 115.17, 103.34, 82.70, 81.00, 67.37, 67.17, 30.53. HRMS (ESI)  $m/z$  calcd for  $\text{C}_{17}\text{H}_{16}\text{FN}_3\text{O}$  298.1356, found 298.1360 [M + H]<sup>+</sup>.

#### 4.6. 2-(4-(2-(2-(2-Fluoroethoxy)ethoxy)ethoxy)phenyl)-N-methylquinoxalin-6-amine (**4b**)

The reaction described for **4a** was used, and 27 mg of **4b** was obtained in a yield of 35.0%.  $^1\text{H}$  NMR (400 MHz,  $\text{CDCl}_3$ )  $\delta$  9.09 (s, 1H), 8.06 (d,  $J$  = 8.6 Hz, 2H), 7.86 (d,  $J$  = 9.0 Hz, 1H), 7.12 (dd,  $J$  = 9.1, 2.1 Hz, 1H), 7.06 (d,  $J$  = 8.6 Hz, 2H), 6.98 (d,  $J$  = 1.7 Hz, 1H), 4.65–4.62 (m, 1H), 4.53–4.50 (m, 1H), 4.24–4.20 (m, 2H), 3.93–3.90 (m, 2H), 3.82–3.79 (m, 1H), 3.78–3.72 (m,  $J$  = 12.5, 4.9 Hz, 6H), 3.00 (s, 3H).  $^{13}\text{C}$  NMR (100 MHz,  $\text{CDCl}_3$ )  $\delta$  158.85, 148.76, 146.25, 142.55, 141.65, 136.08, 129.22, 128.93, 127.12, 121.08, 114.11, 102.12, 82.96, 81.29, 69.90, 69.86, 69.55, 69.35, 68.77, 66.55, 29.49. HRMS (ESI)  $m/z$  calcd for  $\text{C}_{21}\text{H}_{25}\text{FN}_3\text{O}_3$  386.1880, found 386.1891 [M + H]<sup>+</sup>.

#### 4.7. 2-(4-(6-(Methylamino)quinoxalin-2-yl)phenoxy)ethyl 4-methylbenzenesulfonate (**5a**)

A mixture of compound **3** (0.4 mmol), ethane-1,2-diyl bis(4-methylbenzenesulfonate) (0.6 mmol) and  $\text{K}_2\text{CO}_3$  (1.2 mmol) in acetone (10 mL) was refluxed for 10 h, in which 18-Crown-6 was added as catalyzer. After the solvent being removed in vacuo, the residue was purified by silica gel chromatography (petroleum ether/ethylacetate = 1:2) to give 49.4 mg of **5a** in a yield of 27.5%.  $^1\text{H}$  NMR (400 MHz,  $\text{CDCl}_3$ )  $\delta$  9.08 (s, 1H), 8.04 (d,  $J$  = 8.8 Hz, 2H), 7.85 (t,  $J$  = 8.4 Hz, 3H), 7.36 (d,  $J$  = 8.0 Hz, 2H), 7.13 (dd,  $J$  = 9.1, 2.6 Hz, 1H), 6.98 (d,  $J$  = 2.4 Hz, 1H), 6.93 (d,  $J$  = 8.8 Hz, 2H), 4.42 (dd,  $J$  = 5.5, 3.9 Hz, 2H), 4.24 (d,  $J$  = 4.9 Hz, 2H), 3.00 (s, 3H), 2.45 (s, 3H). MS (ESI)  $m/z$  calcd for  $\text{C}_{24}\text{H}_{23}\text{N}_3\text{O}_4\text{S}$  449.1, found 449.6 [M + H]<sup>+</sup>.

#### 4.8. 2-(2-(2-(4-(6-(Methylamino)quinoxalin-2-yl)phenoxy)ethoxy)ethoxy)ethyl 4-methylbenzenesulfonate (**5b**)

The reaction described for **5a** was used, and 210 mg of **5b** was obtained in a yield of 73.6%.  $^1\text{H}$  NMR (400 MHz,  $\text{CDCl}_3$ )  $\delta$  9.09 (s, 1H), 8.06 (d,  $J$  = 8.7 Hz, 2H), 7.85 (d,  $J$  = 9.0 Hz, 1H), 7.80 (d,  $J$  = 8.2 Hz, 2H), 7.32 (d,  $J$  = 8.1 Hz, 2H), 7.13 (dd,  $J$  = 9.1, 2.5 Hz, 1H), 7.05 (d,  $J$  = 8.8 Hz, 2H), 6.97 (d,  $J$  = 2.4 Hz, 1H), 4.21–4.15 (m,  $J$  = 6.4, 5.0 Hz, 4H), 3.89–3.84 (m, 2H), 3.73–3.67 (m, 4H), 3.66–3.62 (m,  $J$  = 5.9, 3.1 Hz, 2H), 2.99 (s, 3H), 2.42 (s, 3H). MS (ESI)  $m/z$  calcd for  $\text{C}_{28}\text{H}_{32}\text{N}_3\text{O}_6\text{S}$  538.2, found 538.5 [M + H]<sup>+</sup>.

#### 4.9. 2-(4-(6-(tert-Butoxycarbonyl)quinoxalin-2-yl)phenoxy)ethyl 4-methylbenzenesulfonate (**6a**)

Compound **5a** (0.1 mmol) was added to a solution of di-tert-butyl dicarbonate (0.4 mmol) and DIEA (0.2 mmol) in THF, and the reaction mixture was refluxed over night. After the solvent being removed in vacuum, the residue was purified by silica gel chromatography (petroleum ether/ethylacetate = 1:1) to give 24 mg of **6a** in a yield of 43.1%.  $^1\text{H}$  NMR (400 MHz,  $\text{CDCl}_3$ )  $\delta$  9.24 (s, 1H), 8.12 (d,  $J$  = 8.6 Hz, 2H), 8.03 (d,  $J$  = 8.9 Hz, 1H), 7.90–7.76 (m, 4H), 7.36 (d,  $J$  = 8.0 Hz, 2H), 6.96 (d,  $J$  = 8.6 Hz, 2H), 4.46–4.39 (m, 2H), 4.29–4.21 (m, 2H), 3.43 (s, 3H), 2.46 (s, 3H), 1.50 (s, 9H). MS (ESI)  $m/z$  calcd for  $\text{C}_{29}\text{H}_{31}\text{N}_3\text{O}_6\text{S}$  549.2, found 549.7 [M + H]<sup>+</sup>.

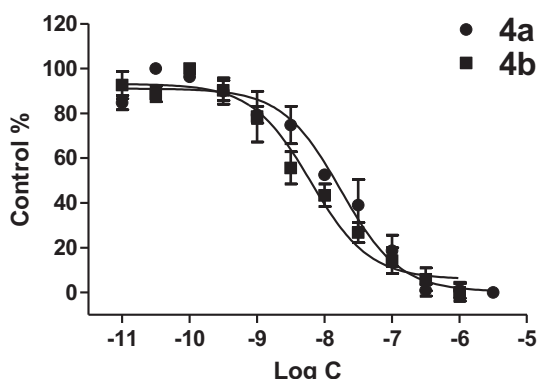


**Fig. 4.** Inhibition curves for the binding of [ $^{125}\text{I}$ ]IMPY to  $\text{A}\beta_{1-42}$  aggregates.

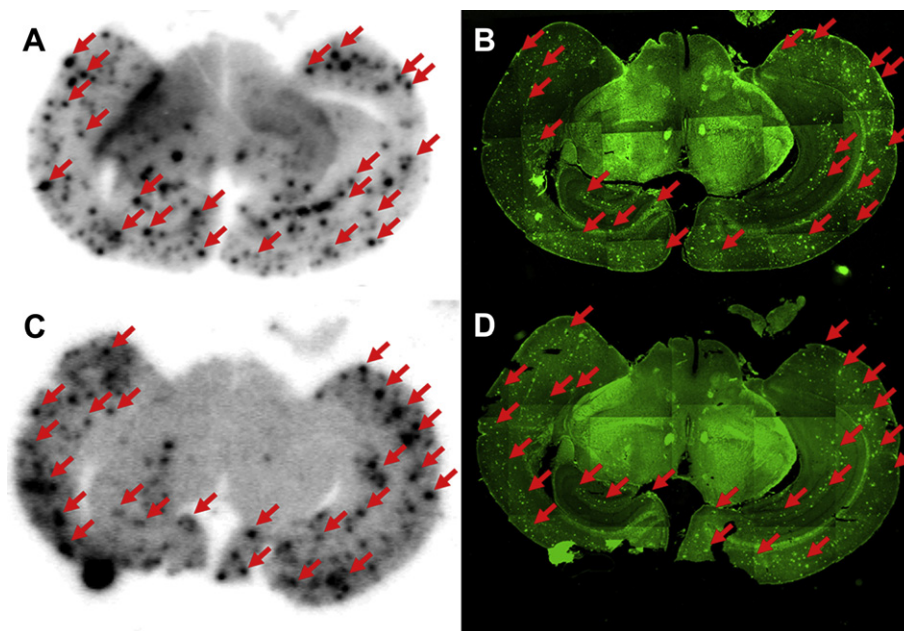


**Fig. 5.** *In vitro* autoradiography of [ $^{18}\text{F}$ ]4a and [ $^{18}\text{F}$ ]4b (A, C) on a Tg model mouse (C57BL6, APP<sup>swe</sup>/PSEN1, 12 months old, male). The presence and distribution of plaques in the sections were confirmed by fluorescence staining using thioflavin-S on the same sections with a filter set for GFP (B, D).

#### 4.10. 2-(2-(2-(4-(6-(tert-Butoxycarbonyl)quinoxalin-2-yl)phenoxy)ethoxy)ethyl 4-methylbenzenesulfonate (**6b**)

The reaction described for **6a** was used, and 67 mg of **6b** was obtained in a yield of 52.6%.  $^1\text{H NMR}$  (400 MHz,  $\text{CDCl}_3$ )  $\delta$  9.25 (s, 1H), 8.15 (d,  $J = 8.8$  Hz, 2H), 8.03 (d,  $J = 9.0$  Hz, 1H), 7.85 (d,  $J = 2.3$  Hz, 1H), 7.83–7.77 (m, 3H), 7.32 (d,  $J = 8.0$  Hz, 2H), 7.08 (d,  $J = 8.9$  Hz, 2H), 4.22–4.16 (m, 4H), 3.90–3.85 (m, 2H), 3.73–3.68 (m, 4H), 3.66–3.61 (m, 2H), 3.43 (s, 3H), 2.42 (s, 3H), 1.50 (s, 9H). MS (ESI)  $m/z$  calcd for  $\text{C}_{33}\text{H}_{39}\text{N}_3\text{O}_6\text{S}$  637.2, found 637.7 [ $\text{M} + \text{H}$ ] $^+$ .

#### 4.11. Radiolabeling

[ $^{18}\text{F}$ ]Fluoride trapped on a QMA cartridge was eluted with 1 mL of Kryptofix 222/ $\text{K}_2\text{CO}_3$  solution. The solvent was removed at 110 °C under a stream of nitrogen gas. The residue was azeotropically dried with 1 mL of anhydrous acetonitrile twice at 110 °C under a stream of nitrogen gas. A solution of tosylate precursor

(1 mg) in 1 mL  $\text{CH}_3\text{CN}$  was added to the reaction tube containing dried [ $^{18}\text{F}$ ] activities. The mixture was heated at 110 °C under nitrogen protecting for 5 min. 200  $\mu\text{L}$  HCl (1 M) was added into the tube and the mixture was heated for another 5 min at 110 °C under nitrogen protecting for deprotection, and neutralized by  $\text{NaHCO}_3$  after being cooled down to room temperature. Water (5 mL) was added, and the mixture was passed through a preconditioned Sep-Pak Plus-C18 cartridge (Waters), which was washed with 10 mL water later. The [ $^{18}\text{F}$ ] labeled compound was eluted with 2 mL of acetonitrile, and purified by HPLC. The [ $^{18}\text{F}$ ] labeled [ $^{18}\text{F}$ ]4a and [ $^{18}\text{F}$ ]4b were prepared with an average radiochemical yield of 20% and 52% (no decay corrected), and radiochemical purity of >98%.

#### 4.12. Binding assay *in vitro* using $\text{A}\beta_{1-42}$ aggregates

Inhibition experiments were carried out in 12  $\times$  75 mm borosilicate glass tubes according to procedures described previously with some modifications. The radio-ligand [ $^{125}\text{I}$ ]IMPY was prepared

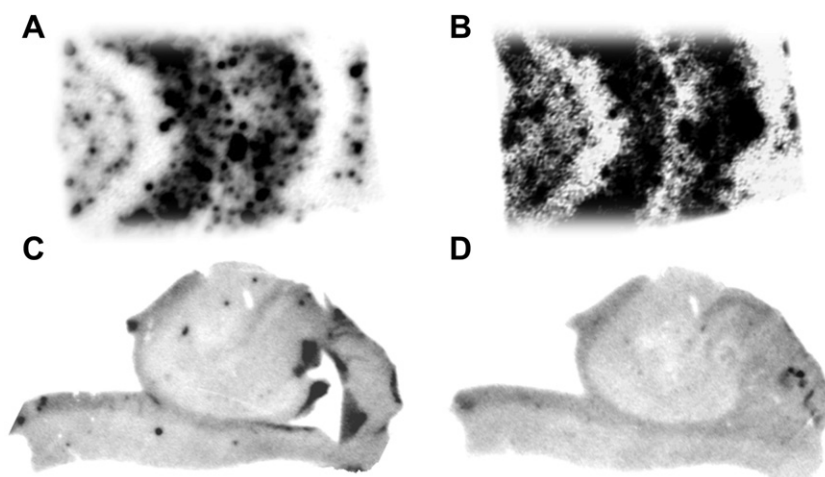


**Fig. 6.** *In vitro* autoradiography of [ $^{18}\text{F}$ ]4a and [ $^{18}\text{F}$ ]4b on AD human brain sections (A, B) and control human brain sections (C, D).

according to procedures described previously [25], after HPLC purification, the radiochemical purity was greater than 95%. For the inhibition assay, 100  $\mu\text{L}$   $\text{A}\beta_{1-42}$  aggregates solution, 100  $\mu\text{L}$  [ $^{125}\text{I}$ ] IMPY solution, 100  $\mu\text{L}$  BSA solution (1%) and 100  $\mu\text{L}$  inhibitors ( $10^{-4}$ – $10^{-9.5}$  M) were added into borosilicate glass tubes. The mixture was incubated at 37  $^{\circ}\text{C}$  for 2 h, and the free radioactivity were separated by vacuum filtration through Whatman GF/B filters using a Brandel Mp-48T cell harvester followed by  $3 \times 4$  mL washes with PBS (0.02 M, pH 7.4) at room temperature. Filters with the bound [ $^{125}\text{I}$ ]IMPY were counted in gamma counter (WALLAC/Wizard 1470, USA) with 70% efficiency. Inhibition experiments were repeated three times, and the half maximal inhibitory concentration ( $IC_{50}$ ) was determined using GraphPad Prism 4.0, and the inhibition constant ( $K_i$ ) was calculated using the Cheng–Prusoff equation:  $K_i = IC_{50}/(1 + [L]/K_d)$  [29]

#### 4.13. Autoradiography *in vitro* using brain sections of human and transgenic model mouse

Paraffin-embedded brain sections were deparaffinized with  $2 \times 20$  min washes in xylene;  $2 \times 5$  min washes in 100% ethanol; a 5 min wash in 90% ethanol/ $\text{H}_2\text{O}$ ; a 5 min wash in 80% ethanol/ $\text{H}_2\text{O}$ ; a 5 min wash in 60% ethanol/ $\text{H}_2\text{O}$  and a 10 min wash in running tap water, and then incubated in PBS (0.2 M, pH = 7.4) for 30 min. The sections were incubated with [ $^{18}\text{F}$ ]4a, [ $^{18}\text{F}$ ]4b (1.85 MBq/200  $\mu\text{L}$ ) for 1 h at room temperature. They were then washed in 40% EtOH, before being rinsed with water for 1 min. After drying, the sections were exposed to a phosphorus plate (PerkinElmer, USA) for 2 h. *In vitro* autoradiographic images were obtained using a phosphor imaging system (Cyclone, Packard). After autoradiographic examination, the same mouse brain sections were stained by thioflavin-S to confirm the presence of  $\text{A}\beta$  plaques. For the staining of thioflavin-S, sections were immersed in a 0.125% thioflavin-S solution containing 10% EtOH for 3 min and washed in 40% EtOH. After drying, the fluorescent observation was performed by the LSM 510 META (Zeiss, Germany) equipped with a LP 505 filter set (excitation, 405 nm; long-pass filter, 505 nm).

#### 4.14. Biodistribution experiments in normal mice

A saline (0.1 mL, 10% EtOH) solution containing  $^{18}\text{F}$ -labeled tracer (370 kBq) was injected into the tail vein of ICR mice (five weeks, 20–22 g, male). The mice ( $n = 5$  for each time point) were executed by decollation at designated time points post injection. The organs of interest were removed and weighed, and radioactivity was counted with an automatic gamma counter (WALLAC/Wizard 1470, USA). The percent dose per gram (%ID/g) of wet tissue was calculated by a comparison of the tissue counts to suitably diluted aliquots of the injected material.

#### 4.15. Partition coefficient determination

The  $^{18}\text{F}$ -labeled tracer (740 kBq) was added to a premixed suspension containing 3 g of *n*-octanol and 3 g of PBS (0.05 M, pH = 7.4) in a test tube. The test tube was vortexed for 3 min at room temperature, and centrifuged for 5 min at 3000 rpm. Two weighed samples from the *n*-octanol (100  $\mu\text{L}$ ) and buffer (500  $\mu\text{L}$ ) layers were measured. The partition coefficient was expressed as the logarithm of the ratio of the count per gram from *n*-octanol versus PBS. Samples from the *n*-octanol layer were repartitioned until consistent partition coefficient values were obtained. The measurement was done in triplicate and repeated three times.

## Acknowledgments

The authors thank Dr. Jin Liu (College of Life Science, Beijing Normal University) for assistance in the *in vitro* neuropathological staining. This work was funded by NSFC (21071023).

## Appendix A. Supplementary information

Supplementary data related to this article can be found at <http://dx.doi.org/10.1016/j.ejmech.2012.08.031>.

## References

- [1] J.A. Hardy, G.A. Higgins, Alzheimer's disease: the amyloid cascade hypothesis, *Science* 256 (1992) 184–185.
- [2] D.J. Selkoe, The origins of Alzheimer disease: a is for amyloid, *JAMA: the Journal of the American Medical Association* 283 (2000) 1615–1617.
- [3] J. Hardy, D.J. Selkoe, The amyloid hypothesis of Alzheimer's disease: progress and problems on the road to therapeutics, *Science* 297 (2002) 353–356.
- [4] C.C. Rowe, V.L. Villemagne, Brain amyloid imaging, *Journal of Nuclear Medicine* 52 (2011) 1733–1740.
- [5] D.J. Selkoe, Imaging Alzheimer's amyloid, *Nature Biotechnology* 18 (2000) 823–824.
- [6] L. Cai, R.B. Innis, V.W. Pike, Radioligand development for PET imaging of beta-amyloid (A $\beta$ ) – current status, *Current Medicinal Chemistry* 14 (2007) 19–52.
- [7] H.F. Kung, S.R. Choi, W. Qu, W. Zhang, D. Skovronsky, 18F stilbenes and styrylpyridines for PET imaging of A beta plaques in Alzheimer's disease: a miniperspective, *Journal of Medicinal Chemistry* 53 (2010) 933–941.
- [8] C.A. Mathis, Y. Wang, W.E. Klunk, Imaging beta-amyloid plaques and neurofibrillary tangles in the aging human brain, *Current Pharmaceutical Design* 10 (2004) 1469–1492.
- [9] C.A. Mathis, Y. Wang, D.P. Holt, G.F. Huang, M.L. Debnath, W.E. Klunk, Synthesis and evaluation of 11C-labeled 6-substituted 2-arylbenzothiazoles as amyloid imaging agents, *Journal of Medicinal Chemistry* 46 (2003) 2740–2754.
- [10] W.E. Klunk, H. Engler, A. Nordberg, Y. Wang, G. Blomqvist, D.P. Holt, M. Bergstrom, I. Savitcheva, G.F. Huang, S. Estrada, B. Aussen, M.L. Debnath, J. Barletta, J.C. Price, J. Sandell, B.J. Lopresti, A. Wall, P. Koivisto, G. Antoni, C.A. Mathis, B. Langstrom, Imaging brain amyloid in Alzheimer's disease with Pittsburgh compound-B, *Annals of Neurology* 55 (2004) 306–319.
- [11] M. Ono, A. Wilson, J. Nobrega, D. Westaway, P. Verhoeff, Z.P. Zhuang, M.P. Kung, H.F. Kung, 11C-Labeled stilbene derivatives as A $\beta$ -aggregate-specific PET imaging agents for Alzheimer's disease, *Nuclear Medicine and Biology* 30 (2003) 565–571.
- [12] N.P. Verhoeff, A.A. Wilson, S. Takeshita, L. Trop, D. Hussey, K. Singh, H.F. Kung, M.P. Kung, S. Houle, In-vivo imaging of Alzheimer disease beta-amyloid with [ $^{11}\text{C}$ ]SB-13 PET, *The American Journal of Geriatric Psychiatry* 12 (2004) 584–595.
- [13] A.E. Johnson, F. Jeppsson, J. Sandell, D. Wensbo, J.A. Neelissen, A. Aureus, P. Strom, H. Norman, L. Farde, S.P. Svensson, AZD2184: a radioligand for sensitive detection of beta-amyloid deposits, *Journal of Neurochemistry* 108 (2009) 1177–1186.
- [14] S. Nyberg, M.E. Jonhagen, Z. Cselenyi, C. Halldin, P. Julin, H. Olsson, Y. Freund-Levi, J. Andersson, K. Varnas, S. Svensson, L. Farde, Detection of amyloid in Alzheimer's disease with positron emission tomography using [ $^{11}\text{C}$ ]AZD2184, *European Journal of Nuclear Medicine and Molecular Imaging* 36 (2009) 1859–1863.
- [15] J.D. Andersson, K. Varnas, Z. Cselenyi, B. Gulyas, D. Wensbo, S.J. Finnema, B.M. Swahn, S. Svensson, S. Nyberg, L. Farde, C. Halldin, Radiosynthesis of the candidate beta-amyloid radioligand [(11C)AZD2184]: positron emission tomography examination and metabolite analysis in cynomolgus monkeys, *Synapse* 64 (2010) 733–741.
- [16] C.C. Rowe, U. Ackerman, W. Browne, R. Mulligan, K.L. Pike, G. O'Keefe, H. Tochon-Danguy, G. Chan, S.U. Berlangieri, G. Jones, K.L. Dickinson-Rowe, M.P. Kung, W. Zhang, M.P. Kung, D. Skovronsky, T. Dyrks, G. Holl, S. Krause, M. Friebe, L. Lehman, S. Lindemann, L.M. Dinkelborg, C.L. Masters, V.L. Villemagne, Imaging of amyloid beta in Alzheimer's disease with 18F-BAY94-9172, a novel PET tracer: proof of mechanism, *Lancet Neurology* 7 (2008) 129–135.
- [17] G.J. O'Keefe, T.H. Saunderson, S. Ng, U. Ackerman, H.J. Tochon-Danguy, J.G. Chan, S. Gong, T. Dyrks, S. Lindemann, G. Holl, L. Dinkelborg, V. Villemagne, C.C. Rowe, Radiation dosimetry of beta-amyloid tracers 11C-PiB and 18F-BAY94-9172, *Journal of Nuclear Medicine* 50 (2009) 309–315.
- [18] M. Koole, D.M. Lewis, C. Buckley, N. Nelissen, M. Vandenbulcke, D.J. Brooks, R. Vandenbergh, K. Van Laere, Whole-body biodistribution and radiation dosimetry of 18F-GE067: a radioligand for *in vivo* brain amyloid imaging, *Journal of Nuclear Medicine* 50 (2009) 818–822.
- [19] S.R. Choi, G. Golding, Z. Zhuang, W. Zhang, N. Lim, F. Hefti, T.E. Beneditum, M.R. Kilbourn, D. Skovronsky, H.F. Kung, Preclinical properties of 18F-AV-45: a PET agent for A $\beta$  plaques in the brain, *Journal of Nuclear Medicine* 50 (2009) 1887–1894.

- [20] K.J. Lin, W.C. Hsu, I.T. Hsiao, S.P. Wey, L.W. Jin, D. Skovronsky, Y.Y. Wai, H.P. Chang, C.W. Lo, C.H. Yao, T.C. Yen, M.P. Kung, Whole-body biodistribution and brain PET imaging with [<sup>18</sup>F]AV-45, a novel amyloid imaging agent – a pilot study, *Nuclear Medicine and Biology* 37 (2010) 497–508.
- [21] D.F. Wong, P.B. Rosenberg, Y. Zhou, A. Kumar, V. Raymont, H.T. Ravert, R.F. Dannals, A. Nandi, J.R. Brasic, W. Ye, J. Hilton, C. Lyketsos, H.F. Kung, A.D. Joshi, D.M. Skovronsky, M.J. Pontecorvo, *In vivo* imaging of amyloid deposition in Alzheimer disease using the radioligand 18F-AV-45 (florbetapir [corrected] F 18), *Journal of Nuclear Medicine* 51 (2010) 913–920.
- [22] A. Jureus, B.M. Swahn, J. Sandell, F. Jeppsson, A.E. Johnson, P. Johnstrom, J.A. Neelissen, D. Sunnemark, L. Farde, S.P. Svensson, Characterization of AZD4694, a novel fluorinated Abeta plaque neuroimaging PET radioligand, *Journal of Neurochemistry* 114 (2010) 784–794.
- [23] M. Cui, M. Ono, H. Kimura, B. Liu, H. Saji, Novel quinoxaline derivatives for *in vivo* imaging of beta-amyloid plaques in the brain, *Bioorganic & Medicinal Chemistry Letters* 21 (2011) 4193–4196.
- [24] K.A. Stephenson, R. Chandra, Z.P. Zhuang, C. Hou, S. Oya, M.P. Kung, H.F. Kung, Fluoro-pegylated (FPEG) imaging agents targeting Abeta aggregates, *Bioconjugate Chemistry* 18 (2007) 238–246.
- [25] M.P. Kung, C. Hou, Z.P. Zhuang, B. Zhang, D. Skovronsky, J.Q. Trojanowski, V.M. Lee, H.F. Kung, IMPY: an improved thioflavin-T derivative for *in vivo* labeling of beta-amyloid plaques, *Brain Research* 956 (2002) 202–210.
- [26] Z.P. Zhuang, M.P. Kung, A. Wilson, C.W. Lee, K. Plossl, C. Hou, D.M. Holtzman, H.F. Kung, Structure–activity relationship of imidazo[1,2-*a*]pyridines as ligands for detecting beta-amyloid plaques in the brain, *Journal of Medicinal Chemistry* 46 (2003) 237–243.
- [27] A.B. Newberg, N.A. Wintering, K. Plossl, J. Hochold, M.G. Stabin, M. Watson, D. Skovronsky, C.M. Clark, M.P. Kung, H.F. Kung, Safety, biodistribution, and dosimetry of <sup>123</sup>I-IMPY: a novel amyloid plaque-imaging agent for the diagnosis of Alzheimer's disease, *Journal of Nuclear Medicine* 47 (2006) 748–754.
- [28] M. Cui, M. Ono, H. Kimura, B. Liu, H. Saji, Synthesis and structure-affinity relationships of novel dibenzylideneacetone derivatives as probes for beta-amyloid plaques, *Journal of Medicinal Chemistry* 54 (2011) 2225–2240.
- [29] Y. Cheng, W.H. Prusoff, Relationship between the inhibition constant (K<sub>1</sub>) and the concentration of inhibitor which causes 50 per cent inhibition (I<sub>50</sub>) of an enzymatic reaction, *Biochemical Pharmacology* 22 (1973) 3099–3108.